

Complementarity Assessment of South Greenland Katabatic Flows and West Europe Wind Regimes

David Radu*, Mathias Berger*, Raphaël Fonteneau*, Simon Hardy*, Xavier Fettweis†, Marc Le Du‡, Patrick Panciatici‡, Lucian Balea‡, Damien Ernst*

*Montefiore Institute, Dept. of Electrical Engineering and Computer Science, University of Liège, Belgium

†Laboratory of Climatology, Dept. of Geography, University of Liège, Belgium

‡R&D Department, Réseau de Transport d'Électricité (RTE), France

Abstract—Current global environmental challenges require firm, yet diverse resolutions in the energy sector. One promising solution consists in harnessing high-quality variable renewable energy (VRE) resources in remote locations, while using transmission links to wheel the power towards end users. In this context, a comparison of western Europe and Greenland wind regimes is proposed. By leveraging a regional atmospheric model with proven results in polar conditions, local climate associated with southern Greenland is identified to exhibit specific characteristics that facilitate extensive VRE generation levels. A methodology to assess the added value of wind harnessing in remote locations is introduced and applied on the aforementioned case study, showing superior and complementary wind generation potential in this region of Greenland with respect to selected European sites.

Index Terms—wind energy, large-scale interconnection, global grid, Europe, Greenland

I. INTRODUCTION

A current trend in the power system community addresses renewable energy harvesting in remote, yet resource-rich locations and their subsequent integration via large-scale interconnections. In a future power system context defined by dominant VRE generation and increased shares of electrical loads, linking separate power systems offers benefits on various operational levels. From a generation standpoint, one may see the potential of VRE harnessing in resourceful sites and subsequent delivery to major load centres via adequate transmission links. In addition, the negative impact that high VRE generation intermittency has on the operation of power systems could be reduced effectively through complementary production profiles originated from different resource patterns arising from time zone difference (on various latitudes) and the timing of seasons (across different longitudes). From a load perspective, exploiting shifted consumption patterns between regions induced by the geographical positioning of the consumers at different longitudes and latitudes has the potential to level out aggregated load profiles. These would, in turn, lead towards a less challenging operation of power systems, reduction of operational and planning costs, and greenhouse gas emission level mitigation.

Coupling distinct power systems from a country, to a regional and ultimately an intercontinental level would result in a globally interconnected electricity network, or a “global grid”. The idea of a global grid was first proposed in [1], where

the authors envision VRE technologies as crucial in meeting the ever-increasing electricity demand, with high-capacity interconnections being the backbone of the corresponding transmission infrastructure. The same article also describes various operational opportunities emerging from such a large-scale project and it highlights regulatory hurdles likely to arise in such a complex set-up. A more comprehensive, yet still conceptual view on the topic is provided in [2]. The book provides a more detailed assessment of the motivation behind the development of a global grid before mapping specific regions for energy harvesting and routes for long-haul interconnections, and finally discussing the technical innovation required for the successful deployment of this project. Also, an economic dispatch model is the subject of ongoing work for a CIGRE Working Group [3] that is investigating the technical feasibility of a global grid, as well as its economic competitiveness by assessing the trade-off between the cost of interconnectors and the benefits associated with remote VRE harvesting.

In the context of a global electricity interconnection, the scope of this paper is to assess the wind resource complementarity between two adjacent macro-regions as part of the broader global grid: Europe and Greenland. Wind availability in the former is sometimes an issue that leads to increased utilization of balancing units (usually fossil fuel-based generators) and storage capabilities. In this regard, seasonal patterns generally show inferior resource availability during summer time [4], while winter conditions could also display wind resource scarcity coupled with usually low solar irradiance. A resource-rich and load-free region such as Greenland has the potential to provide wind energy to European users in times of local scarcity, while mitigating the balancing and storage requirements.

For the remainder of the paper, Section II documents previous works related to remote VRE harvesting and resource potential assessment. Section III introduces the sources of wind data and briefly discusses local features of wind regimes in Greenland (i.e., katabatic winds) that are favourable for extensive VRE generation. Locations for wind power generation to be investigated are selected in Section IV. Section V details the methodology proposed to study the resource complementarity before results of the Europe-Greenland case study are presented in Section VI. Finally, Section VII concludes the paper and proposes related future research directions.

II. RELATED WORKS

Harnessing renewable energy sources (RES) in remote locations to supply major load centres is not a novel approach, as the available literature reveals. One of the first projects of this kind is the DESERTEC initiative [5], which studies the supply of Mediterranean countries by RES-abundant North African and Middle Eastern (MENA) territories. The project emphasizes the vast potential of solar power in the MENA region that could account for 15% of the electricity demand in Europe by 2050. The same approach is followed in the Gobitec proposal [6]. This programme investigates the potential of harvesting VRE in the resource-rich Gobi Desert and its subsequent delivery to major load centres in China, Japan, South Korea or Russia. The report estimates the cumulated potential of the Gobi Desert in terms of wind and PV installed capacity at 2.6 TW. A GIS-based analysis makes the topic of another study that investigates the technical potential of wind, PV and concentrated solar power (CSP) to cover the full electricity demand of Europe and North Africa by 2050 [7]. An IEA study [8] also documents the theoretical potential of solar power generation in various regions known for their characteristic high solar irradiation, while a more recent article investigates the potential for VRE (e.g., wind and PV) harvesting in Australia to supply major demand centres in East and South-East Asia [9].

On a more distinct note, Greenland has also been the subject of VRE resource analysis for power generation. A first PhD thesis on this topic investigates the potential of wind power generation in Greenland by using a mesoscale atmospheric model to recreate local wind regimes [10]. Certain locations are selected for large-scale wind turbine (e.g., 3 MW units) deployment and the study concludes that, even though the site selection process is highly complex, there is undisputed potential for wind power generation in Greenland. A second PhD thesis on the same subject combines micro- and mesoscale climate modelling for an accurate representation of local wind circulation [11]. The conclusion of the study supports the resource potential of Greenland for wind generation, with specific features of local wind regimes (e.g., semi-permanent occurrence of katabatic flows) found to facilitate increased levels of electricity generation. A work authored by a Nordic consortium also studies the potential of renewable energy sources (e.g., hydro, wind, PV) in Greenland and different interconnection possibilities between the latter and northern Europe [12]. In addition, the author of [13] envisions Arctic regions (e.g., Greenland, Norwegian Sea, Barents Sea) as a next step of wind generation deployment in the North Sea, with a cumulated potential of electricity delivery to Europe and North America estimated at 1800 TWh per year.

In addition to assessing regional VRE resources in terms of electricity generation potential, the current work follows the approach proposed in [14], where inter-regional VRE resource complementarity in both space and time is investigated by means of a parametrised family of scalar indicators. Moreover, the wind resource assessment in Greenland is conducted via a mesoscale climate model proven to accurately replicate wind circulation in polar regions [15].

III. REANALYSIS DATA AND KATABATIC WINDS

The process of wind resource assessment, as proposed in this paper, starts with data acquisition. In this regard, collection of wind signals in Europe and Greenland at hourly resolution and covering the last ten years (i.e., 2008-2017) is achieved via two different sources. The first source, used for data collection in Europe, is the state-of-the-art ERA5 reanalysis [16] developed by the European Centre for Medium-Range Weather Forecasts (ECMWF) through the Copernicus Climate Change Service (C3S). It is an atmospheric reanalysis model¹ that incorporates in situ and satellite observations at high temporal (i.e., down to hourly) and spatial (i.e., $0.28^\circ \times 0.28^\circ$) resolution, at various pressure levels and currently covering the last ten years (i.e., 2008 - present). Within the scope of the current paper, the ERA5 data used here is provided at a height of 100 meters above ground level and the hourly sampling rate chosen for wind potential assessment is achieved via linear interpolation from three-hourly output snapshots. Nevertheless, the limitations of reanalysis models in estimating wind energy potential are reported in the particular case of another reanalysis model (i.e., MERRA2) used in the European context, with significant spatial bias being identified for specific sub-regions [18], partly resulting from the coarse spatial resolution used to model the local or topography-induced winds. A comparison between the two reanalysis models [19] concludes that such tools are not recommended for estimating mean wind speeds for given locations due to their limitations in solving “local variations, especially in more complex terrain”.

In order to overcome the limitations of the aforementioned tools when investigating the wind generation potential of Greenland, wind signals are retrieved from a second source, i.e., the regional MAR (Modèle Atmosphérique Régional) model. MAR is a climate model developed specifically for

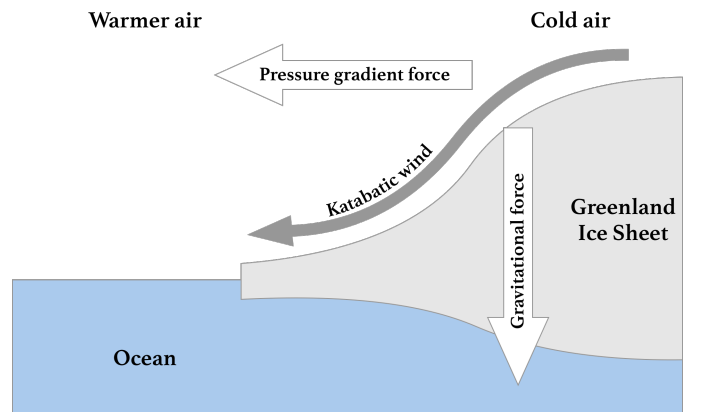


Fig. 1: An illustration of katabatic winds in Greenland, carrying high-density air from a higher elevation down a slope under the force of gravity.

¹Reanalysis is the process of using a data assimilation system (i.e., a sequential procedure in which model states are updated on-line while previous forecasts are continuously compared to available measurements) providing “a consistent reprocessing of meteorological observations” [17].

simulating climatic conditions of polar regions and has been repeatedly validated over Greenland [15]. MAR, as an atmospheric model², solves a set of dynamical equations over a limited integration domain by using reanalysis-based fields (here coming from ERA5) as lateral boundary conditions (e.g., temperature, wind, humidity, pressure at each vertical level of the MAR model). The choice of MAR for estimating Greenland's wind potential is based on its specific ability to accurately represent, at higher resolution (down to $5\text{ km} \times 5\text{ km}$), physical processes in Greenlandic regions, including the local, gravity-driven katabatic winds. For this work, MAR output at hourly resolution is generated at the same altitude level as ERA5 data (i.e., 100 meters above ground level).

The most promising, yet underestimated source of wind generation potential in Greenland stems from the existence of katabatic flows. These local atmospheric movements are the result of heat transfer processes between the cold ice cap and the warmer air mass above it. In brief, when the air mass temperature is higher than that of the ice sheet, the former is cooled down by radiation, thus the air density increases forcing it down the sloping terrain, as depicted in Figure 1. The flow of katabatic winds is driven by gravity, temperature gradient and inclination of the slope of the ice sheet [10]. This wind develops in the first tens of meters above surface (in the boundary layer) with a relatively constant direction down the slope of the terrain, is quasi-constant, but is strengthened when an atmospheric low-pressure area approaches the coast. Katabatic winds develop on a daily basis, regardless of the season, with a slight diurnal shift in their occurrence according to the season (i.e., arrival at the edge of the ice cap during early mornings throughout the winter, around noon during the summer). In addition, the highest intensity of katabatic winds is reported to occur on the south-eastern coast of Greenland, mainly due to steep slopes and flow-channelling conditions [11].

IV. REGION SELECTION

Site selection in Greenland relies on an a priori screening process of the local wind regimes. As seen in Figure 2, Greenland's southernmost region is the most promising from a wind resource perspective, therefore selection of the assessment point is constrained within the yellow and red-coloured areas plotted on the chart, ones with modelled average wind speeds above 13 m/s. In fact, availability of such high average wind speeds is the consequence of the common direction of the general circulation driven winds (as shown on the same chart) and the local katabatic winds that prevents the two atmospheric motions from cancelling each other out. Selection of an onshore point (i.e., GR_{on}) in this area of interest is further supported by year-long high temperatures (associated with low icing risks for the components of wind turbines - Figure 3) and the absence of a permanent ice sheet, as well as by the characteristic low elevation (Figure 4). In addition, an offshore location (i.e., GR_{off}), just south from the onshore one, will be

²An atmospheric model is a mathematical model based on a set of dynamical equations governing atmospheric motions and using numerical methods to obtain approximate solutions of the studied system of coupled equations.

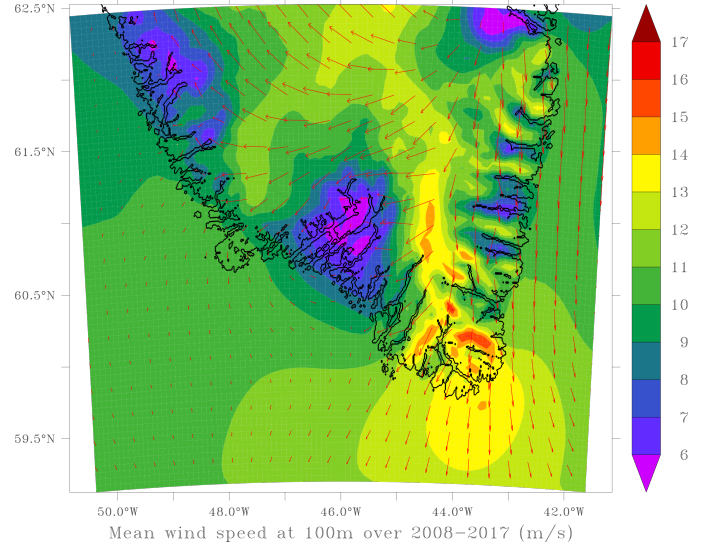


Fig. 2: Greenland average wind speed magnitudes (m/s) as provided by MAR for 2008-2017. Underlying data represents average wind speeds at a 50 m height above ground level and a spatial resolution of $5\text{ km} \times 5\text{ km}$.

assessed. The choice of the latter location is also supported by the bathymetry of Greenland's territorial waters, with depths up to 100 metres. The two sites are marked with a black cross in Figure 3.

Selection of the European generation sites to be compared with the locations in Greenland is initially bound to the region adjacent to or within the North Sea basin, one of the most productive areas on the continent [20]. Within these boundaries, two locations are selected based on the existence of operational wind farms. More specifically, the selected points coincide with the geographical coordinates of the Horns

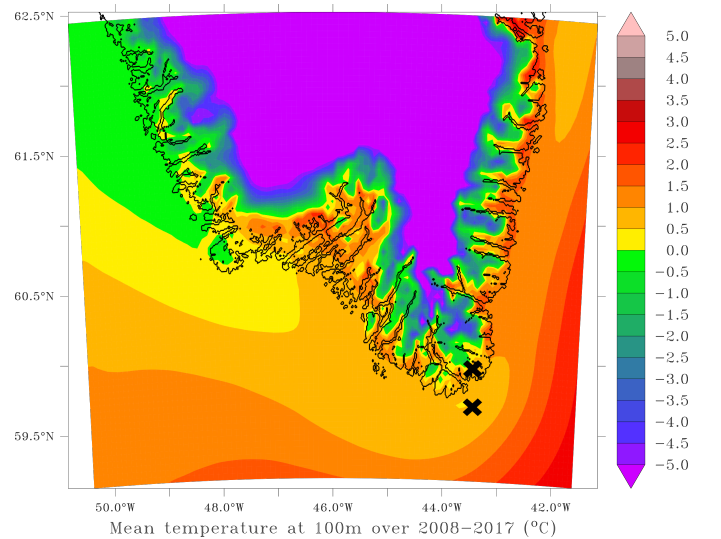


Fig. 3: South Greenland average temperature profiles as computed via MAR for 2008-2017. Underlying data represents annual mean temperature in $^{\circ}\text{C}$ at 100 m above ground level, at a spatial resolution of $5\text{ km} \times 5\text{ km}$.

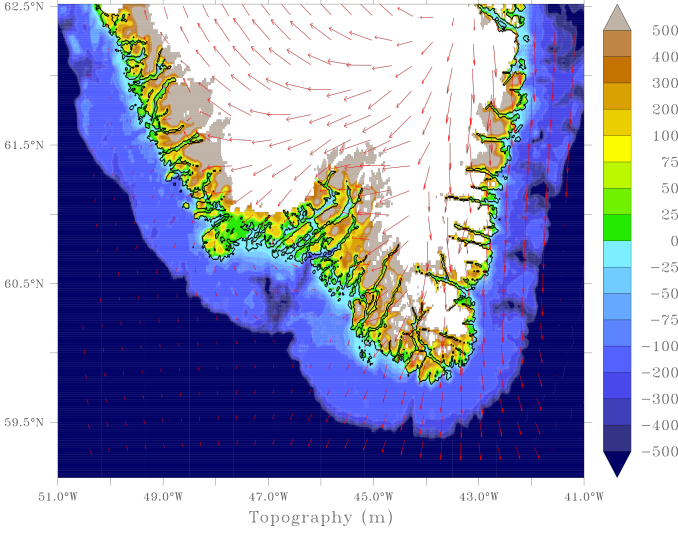


Fig. 4: South Greenland topography superimposed over the land area not covered by permanent ice. Underlying data expressed in metres, at a spatial resolution of $1\text{ km} \times 1\text{ km}$.

Rev (Danish offshore) - DK - and Portes de Bretagne (French onshore) - FR - wind farms. The location of the two wind farms is depicted with a blue cross in Figure 5.

V. METHODOLOGY

A. Wind Time Series: From Magnitude to Complementarity

In this subsection we introduce a method aimed at evaluating the complementarity between wind signals in distinct potential generation sites.

Let \mathcal{L} denote the set of all locations considered, with each particular site $l \in \mathcal{L}$ defined by a pair $l = (\lambda^{lon}, \lambda^{lat}) \in \mathbb{R} \times \mathbb{R}$ of geographical coordinates. Also, let $\mathcal{T} \in \{0, \dots, T-1\}$ represent the time discretisation, where $|\mathcal{T}| = T \in \mathbb{N}$ is the

time horizon. With respect to resource data, we denote by $s_t^l \in \mathbb{R}_{\geq 0}$ a wind signal magnitude sample associated with a specific location $l \in \mathcal{L}$ and a given time stamp $t \in \mathcal{T}$. Two wind speed thresholds are considered, such that v_{low}^{med} is the upper limit of a low wind regime and v_{med}^{high} is the upper bound of a class of moderate winds (Figure 6). Let $\mathcal{S} = \{1, 2, 3\}$ be a set of labels denoting wind regimes and $h : \mathbb{R} \mapsto \mathcal{S}$ be a mapping associating a wind speed class in \mathcal{S} to each resource sample s_t^l , such that:

$$h(s_t^l) = \begin{cases} 1, & s_t^l < v_{min}^{med} \\ 2, & s_t^l \in [v_{min}^{med}, v_{med}^{high}) \\ 3, & s_t^l \geq v_{med}^{high} \end{cases}$$

According to this mapping, any wind time series $s^l \in \mathbb{R}_{\geq 0}^T$ is clustered into three classes, depending on the relative position of each element (s_t^l) with respect to the previously mentioned velocity thresholds. Distribution of wind signals in three classes is suggested here as example, while the proposed clustering method is applicable for any other number of wind signal classes. In this particular case, the sectors correspond to low, medium and high wind regimes. Furthermore, we define a family of mappings $g_{ij} : \mathcal{S} \times \mathcal{S} \mapsto \{0, 1\}$ associating a binary digit value to a pair of wind regime labels, such that:

$$g_{ij}(x, y) = \begin{cases} 1, & (x, y) = (i, j) \\ 0, & \text{otherwise} \end{cases}$$

For any two locations $(l_1, l_2) \in \mathcal{L} \times \mathcal{L}$, we associate a $(|\mathcal{S}| \times |\mathcal{S}|)$ -dimension matrix $M^{(l_1, l_2)}$ with entries:

$$m_{ij}^{(l_1, l_2)} = \frac{1}{T} \sum_{t=0}^{T-1} g_{ij}(h(s_t^{l_1}), h(s_t^{l_2})) \quad (1)$$

We label these m_{ij} values as complementarity factors, each of them being associated with a pair of locations and their corresponding wind class. In brief, a low (high) value of this metric corresponds to a scarce (numerous) occurrence of instances in which the wind regimes for a given pair of locations coincide with classes (i, j) . It is worth noting that both seasonal effects and the stochastic component of wind signals are relevant in evaluating resource complementarity between locations or even extended regions, hence the raw resource data is interpreted as such and thresholds defining wind regimes boundaries are uniform throughout all considered locations. Therefore, complementarity should not be understood in the usual sense of correlation (as computed on detrended signals via standard measures, such as Pearson, Spearman or Kendall correlation coefficients), but rather as the assessment of situations in which system-side, low-generation events occur, a detrimental feature of power systems characterized by high shares of VRE generation.

B. Energy Metrics: From Capacity Factors to Critical Windows

Hereafter, starting from a basic metric (i.e., capacity factor), we carry on with the assessment of wind resource by exploiting the notion of critical time windows [14] for assessing to



Fig. 5: Location of the two European wind farms investigated.

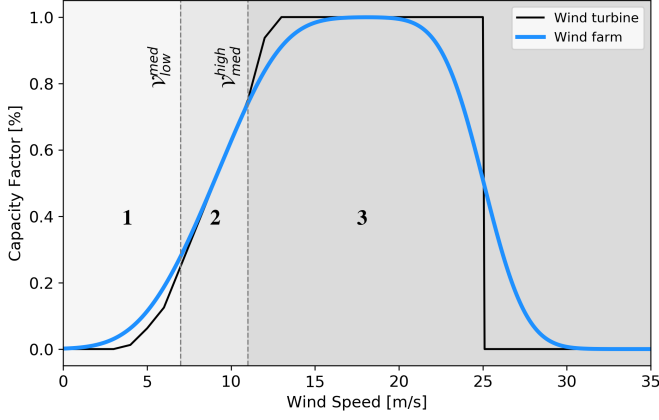


Fig. 6: Single turbine and wind farm transfer functions. Example of wind farm aggregation based on multiple 8MW - aerodyn SCD 8.0/168 units. Wind regimes (1, 2, 3) associated with the two wind speed thresholds - $v_{low}^{med}, v_{med}^{high}$ - also displayed.

which extent aggregating geographical locations may decrease the occurrence of low-generation time periods on a system-wide basis.

1) *Average Capacity Factor*: Let F denote a transfer function associated with a given wind turbine technology. This function maps a hourly average capacity factor for any wind input signal. We also define by $\mathbf{u}^l \in [0, 1]^T$ the capacity factor time series, such that the following component-wise relationship hold:

$$u_t^l = F(s_t^l), \forall l \in \mathcal{L}, \forall t \in \mathcal{T}. \quad (2)$$

Finally, the average capacity factor for a given location can be expressed as:

$$e^l = \frac{1}{T} \sum_{t=1}^T u_t^l, \quad \forall l \in \mathcal{L}. \quad (3)$$

The selection of an appropriate transfer function F is based on a multi-turbine power curve approach proposed in [18] and also used in [14]. In this regard, we make use of an aggregated transfer function modelled via a Gaussian filter (depicted in Figure 6) that emulates the dynamics of a wind farm comprised of identical individual units, while taking as input the wind signal of one single point within this farm.

2) *Critical Time Windows*: Given a time duration $\delta \in \{1, \dots, T\}$, we define a time window w_t^δ as being a set of δ integer(s) starting at time t :

$$w_t^\delta = [t, t + \delta - 1] \cap \mathbb{N}. \quad (4)$$

In addition, the set of all δ -time windows within a time domain that starts at T_s and ends at $T_f > T_s$, such that $(T_f - T_s \geq \delta)$ is denoted as \mathcal{W}^δ and can be further defined as:

$$\mathcal{W}^\delta = \{w_t^\delta | t \in \{T_s, \dots, T_f - \delta\}\}. \quad (5)$$

Note that \mathcal{W}^δ is a set of sets of integers. Also, we introduce a mapping $\hat{U}_\delta : \mathcal{W}^\delta \times [0, 1]^T \mapsto [0, 1]^\delta$ dedicated to extracting

a δ -length truncation of a capacity factor time series \mathbf{u}^l over a time window w_t^δ :

$$\hat{U}_\delta(w_t^\delta, \mathbf{u}^l) = [u_t^l, u_{t+1}^l, \dots, u_{t+\delta-1}^l]. \quad (6)$$

Then, we define a mapping $N_\delta : [0, 1]^\delta \mapsto [0, 1]$ that returns a scalar between zero and one from a δ -long input vector as follows:

$$N_\delta(\mathbf{v}) = \frac{1}{\delta} \sum_{i=1}^{\delta} v_i. \quad (7)$$

In the mapping above, $N_\delta(\mathbf{v})$ represents the average value of the vector $\mathbf{v}(i)$ over its time domain. Let $\alpha \in [0, 1]$ be a capacity factor threshold. For a given location $l \in \mathcal{L}$, we denote by $\Omega_{\delta\alpha}^l$ the set of (δ, α) -critical time windows that gathers all δ -time windows during which the N_δ metric is smaller than α :

$$\Omega_{\delta\alpha}^l = \left\{ w_t^\delta \mid w_t^\delta \in \mathcal{W}^\delta, N_\delta \hat{U}_\delta(w_t^\delta, \mathbf{u}^l) \leq \alpha \right\}. \quad (8)$$

Let $L \in \mathcal{P}(\mathcal{L})$ be a subset of locations. We introduce the set $\xi_{\delta\alpha}(L)$ as being the intersection of (δ, α) -critical time windows over the subset of locations L . Intuitively, such a set contains the time windows during which, wherever the location $l \in L$, the N_δ metric over the considered time window, which corresponds to the average output of the wind farm located at site l , is lower than α :

$$\forall L \in \mathcal{P}(\mathcal{L}), \xi_{\delta\alpha}(L) = \bigcap_{l \in L} \Omega_{\delta\alpha}^l. \quad (9)$$

Finally, we define the last metric for wind resource assessment as a mapping $\Gamma_{\delta\alpha} : \mathcal{P}(\mathcal{L}) \mapsto [0, 1]$:

$$\forall L \in \mathcal{P}(\mathcal{L}), \Gamma_{\delta\alpha}(L) = \frac{\text{card}(\xi_{\delta\alpha}(L))}{\text{card}(\mathcal{W}^\delta)}, \quad (10)$$

where card associates, to any finite set S , the cardinality of S . Concretely, $\Gamma_{\delta\alpha}(L)$ is the proportion of critical δ -time windows within the subset of locations L and considering the measure mapping N_δ .

VI. RESULTS

A. Wind Resource Magnitude Comparison

The descriptive statistics of the wind time series associated with the studied locations are provided in Figure 7. The ten-year mean wind speed in both Greenland locations (i.e., around 14 m/s) is significantly higher than in both European sites (headed by the Danish offshore site, with an average wind speed of close to 10 m/s). In addition, a larger spread of modelled wind speeds in the Greenlandic regions can be observed. We note that, as reported in [21], a high standard deviation of the wind signals usually corresponds to increased turbulence intensity (i.e., short-term wind magnitude fluctuations relative to the mean velocity) that may negatively affect the performance of the wind farm. Nonetheless, it has been observed that larger standard deviation values corresponding to the sites in Greenland are not the result of intra-hourly variations of the underlying wind signal, but are rather due to the strong influence of seasonality of the local natural resource, and may therefore not be associated with high turbulence intensities.

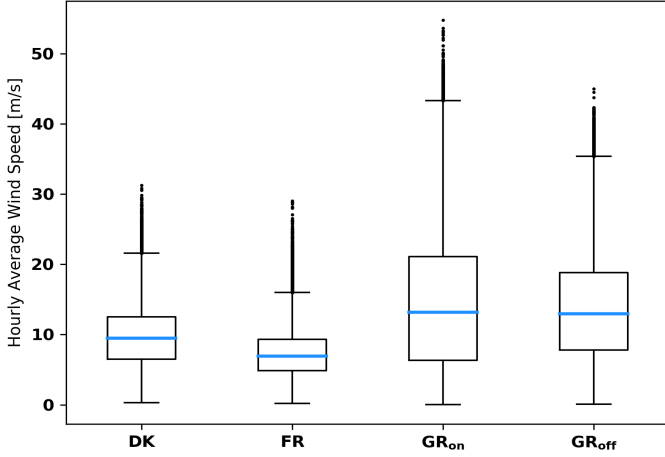


Fig. 7: Boxplots providing descriptive statistics of wind signals for the four locations under consideration.

B. Complementarity of Wind Regimes

Complementarity factors computed on hourly wind signals for the Greenland and European sites are presented in Table I. In this particular case study, velocities associated with different wind regimes are classified into three distinct sectors, bounded by two speed limits ($v_{low}^{med} = 7$ m/s and $v_{med}^{high} = 11$ m/s, respectively), as depicted in Figure 6. Starting with the pairs of neighbouring locations (i.e., DK-FR and GR_{on} - GR_{off} , respectively), one can observe two interesting aspects. Regarding the European sites, it can be seen that 58% of time the wind regimes are low and moderate in both locations, while 36% of the time high winds in one region compensate for low winds in the other. Given the geographical proximity of the two locations in Greenland, the wind regimes in both sites are identical nearly 70% of the time (i.e., sum of elements on the main diagonal). In addition, there is a 50% probability of high wind regimes occurring simultaneously in both Greenlandic locations, a figure that indicates the semi-permanent occurrence of local katabatic wind flows. Looking at values corresponding to the aggregation of European and Greenlandic locations (i.e., DK- GR_{on} , DK- GR_{off} , FR- GR_{on} and FR- GR_{off} , respectively), we observe a clear improvement of the complementarity factors, with at least 50% occurrence of periods of high wind in one location while there are low or moderate winds in the other, regardless of the location pair considered. Moreover, the proportion of time during which wind regimes are simultaneously low or medium drops to approximately half of the values associated solely with the two European locations (i.e., between 26% and 37%, depending on the location pair, versus 58% for DK-FR).

C. Wind Farm Capacity Factor Comparison

Table II shows estimated values for average capacity factors computed as proposed in Section V-B1, assuming a 100% availability of the wind farm (no losses due to icing, down times, etc.). Compared to available operational data, the average capacity factor of the European sites is inflated by approximately 10%, assuming the currently in-use cut-out

TABLE I: Complementarity factors $m_{ij}^{(l_1, l_2)}$ for each pair (l_1, l_2) of considered locations. Two wind speed thresholds define three different classes for low - **1** - (below v_{low}^{med}), intermediate - **2** - (between v_{low}^{med} and v_{med}^{high}) and high - **3** - (above v_{med}^{high}) wind regimes.

FR				GR _{off}					
<div>123</div>				<div>123</div>					
DK	1	0.09	0.11	0.02	GR _{on}	1	0.11	0.10	0.03
	2	0.17	0.21	0.05		2	0.04	0.08	0.07
	3	0.13	0.16	0.06		3	0.01	0.06	0.50

GR _{on}				GR _{off}					
<div>123</div>				<div>123</div>					
DK	1	0.05	0.04	0.12	DK	1	0.04	0.05	0.14
	2	0.11	0.08	0.24		2	0.07	0.10	0.24
	3	0.07	0.07	0.22		3	0.05	0.08	0.23

GR _{on}				GR _{off}					
<div>123</div>				<div>123</div>					
FR	1	0.10	0.07	0.22	FR	1	0.07	0.09	0.22
	2	0.11	0.09	0.28		2	0.08	0.12	0.29
	3	0.03	0.02	0.08		3	0.02	0.03	0.08

speed value of 25 m/s [22], [23]. These overestimates were expected considering the 100% availability assumption and the overestimation in reanalysis models of wind resource potential in northern and western Europe, as reported in [18]. Therefore, given the recurrent validation of MAR in accurately replicating wind conditions in polar regions [15], the differences between the capacity factors in the two Greenlandic locations and the ones associated with the European sites are even greater than those which can be inferred from Table II. The second row of the same table shows the maximum theoretical capacity factor under the assumption that the individual units comprising a wind farm have a cut-out speed superior to any local wind speed to which they are exposed. In this case, while the average capacity factors of the European sites are barely affected (indicating very few occurrences of wind velocities above the current cut-out speeds), the same thing cannot be said about the locations in Greenland. There, under increased cut-out speed conditions, the onshore site would have the highest capacity factor gain (i.e., 15%), while an offshore wind farm could reach capacity factors of almost 70%.

TABLE II: Average capacity factors for the studied wind generation sites considering a transfer function associated with an aggregated wind farm for (i) a cut-out wind speed of 25 m/s and (ii) an ideal cut-out wind speed superior to the maximum wind speed observed at different locations ($max_{l,t} s_t^l$).

v_{cut}^{out} (m/s)	DK	FR	GR _{on}	GR _{off}
25	0.55	0.32	0.49	0.60
$max_{l,t} s_t^l$	0.56	0.33	0.64	0.69

D. Critical Time Windows Analysis

The influence of Greenlandic locations on the (δ, α) critical time windows outcome is detailed in Table III for six capacity factor threshold levels (i.e., from 20% to 70%) and four time window lengths (i.e., one hour, six hours, one day and one week). The first important observation concerns the lower proportion of critical time windows solely for the two sites (in green) in Greenland and for generation thresholds above 20% compared to the values related to the European locations (in black). Selected sites in Greenland are in close proximity and this feature should attract strong non-complementarity in terms of air mass dynamics. However, lower values compared to the aggregation of Europe's two locations suggest better wind potential due to the existence of more constant local wind flows, i.e., the katabatic winds. Moreover, for short time window lengths (one day at most) the gain in terms of critical time window occurrence (i.e., the difference between values linked with the same (δ, α) parameters for the two regions) increases as the generation threshold grows, again indicating superior wind magnitudes associated with the sites in Greenland. Finally, the advantage of coupling the two regions is evident under all considered set-ups. For example, instances when wind production levels for 24 consecutive hours in both Greenland and Europe drop below 70% account for less than one third (i.e., 32%) of the full time frame. These results prove the added value of linking remote regions in terms of both complementarity and magnitude of wind signals.

VII. CONCLUSION AND FUTURE WORK

A systematic assessment of wind regime complementarity in Greenland and western Europe has been conducted. A certain area in southern Greenland is identified to have extensive wind power generation potential and to manifest complementary regimes with respect to European locations known for their high wind energy yield. These results support the key message of the study, according to which tapping into remote areas with extensive renewable energy generation

TABLE III: Values of $\Gamma_{\delta\alpha}$ computed from the intersection of only the two European sites (black), the intersection of only the Greenland sites (green) and for the intersection of all four locations (blue).

$\delta \backslash \alpha$	20%	30%	40%	50%	60%	70%
1	0.11 0.14 0.02	0.18 0.19 0.04	0.27 0.25 0.07	0.35 0.30 0.11	0.44 0.35 0.17	0.53 0.42 0.23
6	0.10 0.12 0.01	0.18 0.18 0.04	0.27 0.24 0.07	0.35 0.30 0.11	0.45 0.37 0.17	0.54 0.44 0.25
24	0.08 0.06 0.01	0.16 0.12 0.02	0.26 0.19 0.06	0.36 0.28 0.11	0.48 0.39 0.20	0.59 0.53 0.32
168	0.01 0.00 0.00	0.06 0.01 0.00	0.18 0.06 0.01	0.38 0.18 0.08	0.58 0.43 0.26	0.77 0.75 0.58

potential can prove beneficial for a secure and reliable supply of electricity in future power systems dominated by VRE. Lastly, technological innovation in wind turbine manufacturing could enable the achievement of even higher capacity factors in Greenlandic regions swept by regular winds of very high velocities.

Regarding further research directions, analysis of wind regimes at different heights above ground level is of considerable interest taking into account the particular features of the katabatic air flow in Greenlandic regions. In this regard, increased average capacity factors are anticipated, even at lower elevations (e.g., 50 metres above ground level), where the higher influence of topography and heat transfer processes bolsters a more frequent occurrence of semi-permanent katabatic flows, while the cut-out speeds of wind converters are reached less often. Another step in assessing VRE resource quality in Greenland and its relevance within a European context includes a tailored cost-benefit analysis intended to quantify the added value of a local Greenlandic wind farm linked with Europe through an HVDC interconnection. In addition, a mapping of various regulatory (e.g., investment mechanisms, remuneration schemes, operational and trading features) and geopolitical aspects is envisioned in order to provide a more complete view of the complexity surrounding the development of interconnectors as part of a global electricity network.

REFERENCES

- [1] S. Chatzivasileiadis, D. Ernst, and G. Andersson, "The global grid," *Renewable Energy*, vol. 57, pp. 372–383, 2013.
- [2] Z. Liu, *Global electricity interconnection*. Academic Press, 2016.
- [3] CIGRE Workgroup C1.35, "Global electricity network feasibility study," 2016.
- [4] G. Ingeborg and M. Korpås, "Variability characteristics of European wind and solar power resources - A review," *Energies*, vol. 9, no. 6, 2016.
- [5] S. Erdle, "The DESERTEC initiative - Powering the development perspectives of Southern Mediterranean countries?" 2010.
- [6] S. Mano, B. Ovgor, Z. Samadov, M. Pudlik, V. Julch, D. Sokolov, and J. Y. Yoon, "Gobitec and Asian Super Grid for renewable energies in Northeast Asia," Energy Charter Secretariat and Energy Economics Institute of the Republic of Korea and Energy Systems Institute of the Russian Federation and Ministry of Energy of Mongolia and Japan Renewable Energy Foundation, 2014.
- [7] W. Platzer, I. Bole, A. Vogel, N. Tham, and P. Bretschneider, "Supergrid study - Approach for the integration of renewable energy in Europe and North Africa," Fraunhofer ISE, 2016.
- [8] K. Komoto, T. Ehara, H. Xu, F. Lv, S. Wang, P. Sinha, E. Cunow, A. Wade, D. Fairman, K. Araki, M. Perez, K. Megherbi, N. Enebish, C. Breyer, and D. Bogdanov, "Energy from the desert: Very large scale PV power plants for shifting to renewable energy future," International Energy Agency (IEA - PVPS Task 8), 2015.
- [9] A. Gulagi, D. Bogdanov, M. Fasihi, and C. Breyer, "Can Australia power the energy-hungry Asia with renewable energy?" *Sustainability*, vol. 9, no. 2, 2017.
- [10] J. P. da Silva Soares, "Wind energy utilization in Arctic climate," Ph.D. dissertation, Uppsala University, 2016.
- [11] K. R. Jakobsen, "Renewable energy potential of Greenland with emphasis on wind resource assessment," Ph.D. dissertation, Technical University of Denmark, 2016.
- [12] Orkustofnun, Norges Arktiske Universitet, Energy Styrlsen, Jærdfeingi, Shetland Islands Council, and Greenland Innovation Centre, "North Atlantic Energy Network," 2016.
- [13] Z. Liu, *Global electricity interconnection*. Academic Press, 2016, ch. Building Global Energy Interconnection.
- [14] M. Berger, D. Radu, R. Fonteneau, R. Henry, M. Glavic, X. Fettweis, M. L. Du, P. Panciatici, L. Balea, and D. Ernst, "Critical time windows for renewable resource complementarity assessment," *Submitted*, 2018.

- [15] X. Fettweis, J. E. Box, C. Agosta, C. Amory, C. Kittel, C. Lang, D. van As, H. Machguth, and H. Gallée, “Reconstructions of the 1900–2015 Greenland ice sheet surface mass balance using the regional climate MAR model,” *The Cryosphere*, vol. 11, pp. 1015–1033, 2017.
- [16] European Centre for Medium-Range Weather Forecasts - ECMWF, “Copernicus knowledge base - ERA5 data documentation,” 2018, <https://confluence.ecmwf.int/display/CKB/>.
- [17] R. Gelaro, W. McCarty, M. J. Suárez, R. Todling, A. Molod, L. Takacs, C. A. Randles, A. Darmenov, M. G. Bosilovich, R. Reichle, K. Wargan, L. Coy, R. Cullather, C. Draper, S. Akella, V. Buchard, A. Conaty, A. M. da Silva, W. Gu, G.-K. Kim, R. Koster, R. Lucchesi, D. Merkova, J. E. Nielsen, G. Partyka, S. Pawson, W. Putman, M. Rienecker, S. D. Schubert, M. Sienkiewicz, and B. Zhao, “The modern-era retrospective analysis for research and applications, version 2 (MERRA-2),” *Journal of Climate*, vol. 30, no. 14, pp. 5419–5454, 2017.
- [18] I. Staffell and S. Pfenninger, “Using bias-corrected reanalysis to simulate current and future wind power output,” *Energy*, vol. 114, pp. 1224–1239, 2016.
- [19] J. Olausson, “ERA5: The new champion of wind power modelling?” *Renewable Energy*, vol. 126, pp. 322–331, 2018.
- [20] European Wind Energy Association - EWEA, “Wind energy scenarios for 2030,” 2015.
- [21] L. J. L. Stival, A. K. Guetter, and F. O. de Andrade, “The impact of wind shear and turbulence intensity on wind turbine power performance,” *Espaço Energia*, pp. 11–20, 2017.
- [22] Danish Energy Agency, “Overview of the energy sector - Master data register of wind turbines,” 2018.
- [23] RTE, “Bilan électrique et perspectives - Bretagne,” 2016.